Sensing and Bio-Sensing Research 7 (2016) 100–106

Contents lists available at ScienceDirect

Sensing and Bio-Sensing Research

journal homepage: www.elsevier.com/locate/sbsr

Impedance spectral fingerprint of *E. coli* cells on interdigitated electrodes: A new approach for label free and selective detection

Maria Mallén-Alberdi [a,b,*], Núria Vigués [c], Jordi Mas [c], César Fernández-Sánchez [a], Antonio Baldi [a]

[a] Instituto de Microelectrónica de Barcelona (IMB-CNM), CSIC, Campus UAB, E-08193 Bellaterra, Spain
[b] Estudis de Doctorat de Biotecnologia, Universitat Autònoma de Barcelona, Campus UAB, E-08193 Bellaterra, Spain
[c] Grup de Microbiologia Ambiental, Universitat Autònoma de Barcelona, Campus UAB, E-08193 Bellaterra, Spain

ARTICLE INFO

Article history:
Received 17 September 2015
Accepted 3 February 2016

Keywords:
Impedance spectroscopy
Bacterial detection
Interdigitated electrodes
Label-free detection
Immuno-detection
E. coli O157:H7

ABSTRACT

Impedance-based biosensors for bacterial detection offer a rapid and cost-effective alternative to conventional techniques that are time-consuming and require specialized equipment and trained users. In this work, a new bacteria detection scheme is presented based on impedance measurements with antibody-modified polysilicon interdigitated electrodes (3 μm pitch, IDEs). The detection approach was carried out taking advantage of the *E. coli* structure which, in electrical terms, is constituted by two insulating cell membranes that separate a conductive cytoplasmatic medium and a more conductive periplasm. Impedance detection of bacteria is usually analyzed using electrical equivalent circuit models that show limitations for the interpretation of such complex cell structure. Here, a differential impedance spectrum representation is used to study the unique fingerprint that arises when bacteria attach to the surface of IDEs. That fingerprint shows the dual electrical behavior, insulating and conductive, at different frequency ranges. In parallel, finite-element simulations of this system using a three-shell bacteria model are performed to explain such phenomena. Overall, a new approach to detect bacteria is proposed that also enables to differentiate viable bacteria from other components non-specifically attached to the IDE surface by just detecting their spectral fingerprints.

1. Introduction

Detection of live bacteria is required for many applications in a wide range of different concentrations, from less than 1 CFU/mL in food and drinking water control to hundreds of CFU/mL in waste water treatment processes [1]. Current standard analytical methods are based on an enrichment phase in a selective media followed by detection of colonies or individual cells. Detection has been traditionally based on time-consuming visual examination, either with naked eye or under microscope [2, 3]. More recently developed methods like automated flow cytometry or most probable number (MPN) approaches rely on optical detection using fluorescence [4].

Impedance based detection is also becoming popular because of its low-cost, versatility and easy implementation in multi-channel systems [5, 6]. The impedance across two electrodes immersed in a solution can be altered in many different ways by the presence of bacteria. For example, the metabolic activity of bacteria can be monitored through changes in the culture media conductivity [7]. Several systems based on this principle are currently available in the market. The presence of cells on the surface of electrodes has also been detected by changes in the interface impedance [8–10]. When no electroactive species are present in the solution, the interface impedance is basically composed of the double layer capacitance in series with the impedance of any material attached to the electrodes. Cells captured at the surface of the electrodes will slightly alter the interface impedance by blocking low frequency currents at the area of contact. Using interdigitated electrodes (IDEs) and impedance spectroscopy techniques also enable measuring the electrical properties of the volume of solution close to the surface [11]. By fitting the impedance spectra of the IDEs to an electrical equivalent circuit (EEC), the resistance and capacitance of the solution between the electrodes can be obtained [12]. The presence of bacteria at the surface alters the value of these EEC components. In this context, selective detection of live *E. coli* cells was demonstrated by measurement of changes in the solution capacitance of antibody-functionalized polysilicon IDEs [13]. However, bacteria cells complex structure do not fit well to an EEC [14], and hence, the use of EEC fitting can easily lead to false interpretation of results in the presence of other interfering phenomena like conductivity changes or unspecific adsorption of other components of the solution to the electrode surface [15].

E. coli DSMZ 17076 was used as model bacteria. *E. coli* are Gram-negative bacillus with average size of 2 μm in length and 0.5 μm in diameter. The structure of these cells comprises an outer membrane, the

* Corresponding autor at: Instituto de Microelectrónica de Barcelona (IMB-CNM), CSIC, Campus UAB, E-08193 Bellaterra, Spain.
E-mail address: Maria.Mallen@imb-cnm.csic.es (M. Mallén-Alberdi).

http://dx.doi.org/10.1016/j.sbsr.2016.02.001

periplasm interspace, the inner membrane and the cytosol. Inside the periplasm there is the cell wall, which is mainly composed of peptidoglycan, a negatively charged polymer. Therefore, in electrical terms, these bacteria are constituted of two insulating cell membranes, a conductive cytoplasmatic medium and a more conductive periplasm.

What we present in this work is the use of a differential impedance spectra representation, instead of the widespread fitting to EEC, to analyze the unique fingerprint that arises when bacteria attach to the surface of IDE transducers. That fingerprint shows the dual electrical behavior, that is insulating and conductive, which is unambiguously detected at different frequency ranges. We also use Finite Element Analysis (FEA) simulations of the, from here on, called electrode-bacteria system to explain the particular features of such fingerprint.

2. Materials and methods

2.1. Chemicals and reagents

Goat anti-*E. coli* O157:H7 (IgG, polyclonal) was obtained from KPL Inc. IgG was conjugated to streptavidin using a commercially available kit (Lightning-Link™ Streptavidin Conjugation Kit) purchased from Innova Biosciences. Glycine, KCl, (3-aminopropyl)trimethoxysilane (APTMS) and bovine serum albumin (BSA), were obtained from Sigma-Aldrich. NHS-PEG_{12}-Biotin derivative was purchased from Thermo Scientific. 1 μm-diameter silica spheres were obtained from Bangs Laboratories Inc.

2.2. Culture and planting of bacteria

The *E. coli* DSMZ strain used in this work is non-pathogenic but phenotypically similar to the toxigenic strain of *E. coli* O157:H7.

Bacteria were grown aerobically in Luria-Bertani broth for 18 h at 37 °C in a shaker bath (160 rpm). Grown cultures were centrifuged for 10 min at 10,100 g (5804R Eppendorf centrifuge, Germany). The supernatant was removed and the resulting cell pellet was resuspended in $2.5 \cdot 10^{-1}$ M glycine buffer pH 6 (adjusted with diluted KCl, 30 S/cm conductivity). The process was repeated twice in order to remove metabolic products, membrane fragments and cytoplasmatic proteins. The final pellet was resuspended in 20 mL of glycine buffer and the optical density was measured at 600 nm in a Smartspec™ Plus spectrophotometer (Bio-rad, California, USA). The obtained optical density was interpolated into a standard curve in order to get the number or cells per milliliter.

2.3. Interdigitated microelectrodes and its surface functionalization

Polysilicon IDEs containing 466 1.5-μm wide fingers, separated 1.5 μm, with an overall interdigitated area of 2.25 mm^2 and produced in-house at the IMB-CNM clean room, were used as the impedimetric transducers. A detailed description of the IDE fabrication process has been reported elsewhere [16]. These were functionalized with specific goat polyclonal antibodies (Ab) to *E. coli*. For that, the IDE surface was initially cleaned and activated by an oxygen plasma treatment (200 W, 0.8 mbar, 2 min in Tepla 300 instrument), and then silanized with APTMS by a chemical vapor deposition approach [17]. Afterwards, biotin was covalently attached to the silanized IDE surface by incubation in a dimethyl sulfoxide solution containing 10 mM NHS-PEG_{12}-Biotin derivative for 30 min at room temperature. Then, the resulting biotinylated IDE surface was rinse thoroughly in pure acetone followed by an incubation in a 0.1 M phosphate buffer (PB) pH 7 solution containing 0.5 μg/mL anti-*E. coli* specific Ab–streptavidin conjugate. Finally, the Ab-coated IDEs were rinsed with PB-T (PB 0.05% Tween) and stored in PB until use. A thorough characterization of every step of the set protocol was carried out by fluorescence imaging and detailed in Supplementary information.

2.4. Experimental setup

Ab-modified polysilicon IDEs were rinsed with glycine $2.5 \cdot 10^{-1}$ M and then immersed in another glycine solution spiked with *E. coli* at a concentration of 10^8 CFU/ml, and whose conductivity was adjusted to a value of $3 \cdot 10^{-3}$ S/m with KCl. Measurements were performed with a SI 1260 Solartron Impedance Analyzer, at 10 mV voltage amplitude, 0 V DC potential, in a frequency range between 1 KHz and 10 MHz and at three set incubation times of 0, 15 and 30 min.

A commercial conductimeter (Crison Micro CM 2202) was used to control changes in solution conductivity during impedance measurements. A slight increase of conductivity hovering around 10% was detected in solutions containing 10^8 CFU/mL *E. coli*, which is likely to be produced by the cell metabolic activity. Conductivity correction was performed for all the data by subtracting the impedance variation recorded with the same IDE in response to equivalent variations of conductivity in a pure KCl solution (detailed explanation at Supplementary information).

Other related events were measured in order to compare its signal to bacterial impedance response:

BSA was adsorbed on the IDE surface by incubation in a 1% BSA (m/v) aqueous solution for 1 h. The impedance spectrum was measured before and after BSA adsorption in the same glycine solution as above.

Silica beads were deposited on the surface of the electrodes by precipitation from a bead suspension prepared in deionized water. The beads were weakly attached to the surface of the IDE by drying them for 5 min at 80 °C in a hotplate. The impedance spectrum was measured in the same glycine solution as above before and after silica bead deposition.

3. Results and discussion

Fig. 1a and b show Bode plots of the Ab-modified polysilicon IDEs immersed in a solution spiked with *E. coli*. Measurements were performed at three set incubation times of 0, 15, and 30 min.

First, the Z magnitude Bode plot exhibits the expected shape with three distinct slopes. At low frequencies ($<10^5$ Hz) the impedance is dominated by the impedance of the electrode-solution interface. In the case of polysilicon IDEs immersed in aqueous solution, this impedance is related to the electrochemical double layer and the native silicon oxide layer. It is of capacitive nature and therefore produces a slope in the spectrum close to −20 db per decade of frequency. At middle frequencies (10^5 to 10^6 Hz), the impedance is dominated by the resistance of the solution between the IDE electrodes which is independent of frequency and inversely proportional to the solution conductivity, thus yielding a slope close to 0 db per decade. At high frequencies ($>10^6$) the spectrum slope is also close to −20 db per decade as the impedance is dominated by the capacitance of the solution, which is proportional to the solution permittivity. At the highest frequency measured (10^7 Hz), a slight decrease of the slope is appreciated. This can be associated to the resistance of the polysilicon electrodes [16].

Once conductivity variations are compensated, as explained above, the impedance changes produced by the cells captured at the IDE surface are too small to be appreciated in the Bode plots. However, if the relative variation of the impedance module and phase are plotted, a clear change in the spectra is detected, as shown in Fig. 1 c and d, this being the bacteria fingerprint in the impedance spectra due to the interaction with the Ab-modified IDE. The relative variation of the impedance was calculated as the normalized value of the increment of the impedance at a set measured time with respect to that recorded at time = 0 (just after the IDE was dipped in the cell solution). In the measured frequency range (10^3 to 10^7 Hz) there are two clear peaks, one at positive and the other at negative values that increase with time as the density of cells on the IDE surface increases. The increase of impedance at low frequencies (first peak) is consistent with previous results obtained for impedimetric detection of bacteria [8, 9]. The second negative

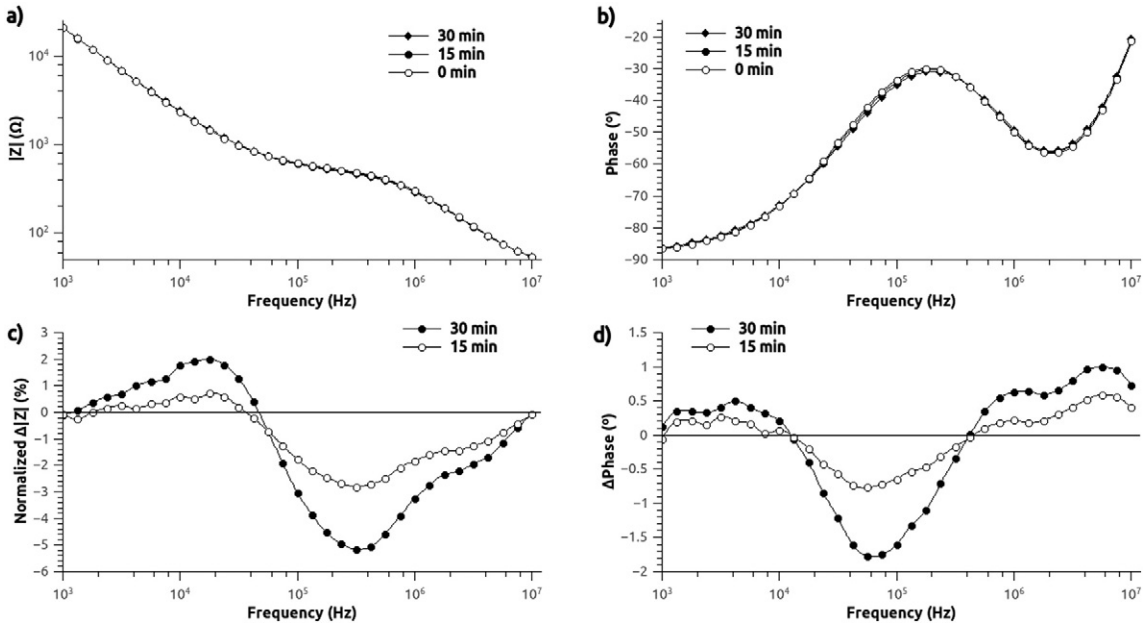

Fig. 1. Bode plots representing impedance modulus (a) and phase (b) as a function of frequency for each measured time; and impedance modulus (c) and phase (d) increments calculated with respect to the measurement recorded at time = 0 min. All graphs were corrected to compensate the conductivity changes in solution taking place during the time frame of the analysis.

peak indicates a decrease of impedance in the middle frequency range, which suggests that the cells are behaving not as insulating but as conducting particles. This is in agreement with a β-dispersion phenomena observed in cell suspensions [18]. Beyond a critical frequency, fc, currents can penetrate through the cell membranes, and the dielectric properties of the cytoplasm (and in turn of the periplasm in gram-negative cells) have an effect on the measured impedance. In the measurements carried out in the present work, the cells are suspended in a solution having a conductivity of $3 \cdot 10^{-3}$ S/m, which is two orders of magnitude lower than the reported cytoplasm conductivity for *E. coli*. Therefore, for a frequency higher than fc, a significant decrease in the measured IDE impedance can be expected.

SEM images of the IDE surface showed that cells were randomly distributed on the IDE surface. Those cells contacting both electrodes produce short-circuit at that frequency range and, as a consequence, they should yield a higher signal than those cells just contacting one of the electrodes.

In addition, the peaks of differential graphics are shown to duplicate its value from 15 to 30 min. These results make evident the ability of this new method to quantify cells as well as specifically distinguish them from other analytes.

To support our hypothesis, the event consisting of a bacterium contacting both IDEs was studied with the help of finite-element simulations (Comsol Multiphysics®). A three-shell model reported by Bai et al. [19] was used to simulate the bacterium. It describes *E. coli* with all its main components and its electrical properties, that is outer membrane ($\varepsilon = 10$, $\sigma = 0$ S/m, thickness = 7 nm), periplasm ($\varepsilon = 60$, $\sigma = 3$ S/m, thickness = 10 nm), inner membrane ($\varepsilon = 6$, $\sigma = 0$ S/m, thickness = 7 nm) and cytoplasm ($\varepsilon = 81$, $\sigma = 0.22$ S/m). A cylinder with hemispherical shells having a radius of 0.25 μm and a total length of 2 μm was chosen as the cell geometry, which is more similar to the real cell shape than the spheroid proposed in Bai's work. Dielectric parameters of the medium were $\varepsilon = 81$ and $\sigma = 3 \cdot 10^{-3}$ S/m. Hence, the impedance of the IDEs was simulated as a capacitance (double layer and native oxide capacitance) and a resistance in series (polysilicon resistance). These parameters show values of $1.7 \cdot 10^{-2}$ F/m^2 and 40 Ω, respectively, when obtained from fitting the equivalent circuit to the experimental impedance spectra.

Figs. 2a and b confirm that at low frequencies (1 kHz) currents do not penetrate the bacterium outer membrane and by contrast, they do so at higher frequencies (1 MHz). That is, at high frequencies bacteria behave as a conductive particle short-circuiting electrodes. Interestingly, at 1 MHz, the bacterium periplasm accounts for 72.29% of the current owing to its higher conductivity despite it only represents 8.5% of the total cross-sectional area of the bacterium.

We also simulated the perturbation that would cause cell shaped particles without membranes that were entirely insulating ($\varepsilon = 1$, $\sigma = 0$ S/m), or entirely conductive ($\varepsilon = 81$, $\sigma = 0.22$ S/m). Likewise, the perturbation of the IDE impedance caused by an arbitrary fixed decrease in the interface capacitance of $5 \cdot 10^{-4}$ F/m^2 was estimated. Simulated spectra obtained for all these cases are plotted in Fig. 3a together with one experimental measurement. From these plots it is clear that impedance increments are related to the particle insulating behavior and decrements are associated to particle conductive behavior. Bacteria exhibit a dual electrical behavior that corroborates our initial hypothesis. Nevertheless, it should be mentioned that the experimental positive peak is larger than that simulated one and starts at lower frequency values. This behavior suggests that cells also produce a change in the interface impedance. An explanation to this phenomenon could be that the buffer used to carry out the measurement shows low conductivity and concentration of nutrients so that it could activate a general stress response to bacteria. This response is a common bacteria behavior that allows them to persist in a wide variety of environments. One of the effects of these stress conditions could be the formation of adhesion structures, such as curli and fimbriae and the secretion of exopolysaccharides [20, 21], which would produce an increase in the IDE interface impedance and that was not taken into consideration in the simulation experiments.

In order to corroborate this explanation, the relative impedance variation spectra was obtained for other related events, namely an increase of media conductivity, the addition of an adsorbed BSA layer at the surface, and the attachment of 1 μm-diameter silica beads. Fig. 3 b shows the curves obtained in each case. For a conductivity increase, from $2.8 \cdot 10^{-3}$ S/m to $3.1 \cdot 10^{-3}$ S/m, the impedance decreases in the middle frequency range similar to the response obtained when conductive particles were simulated. The impedance spectrum was measured before and after BSA adsorption in the same glycine solution ($3 \cdot 10^{-3}$ S/m),

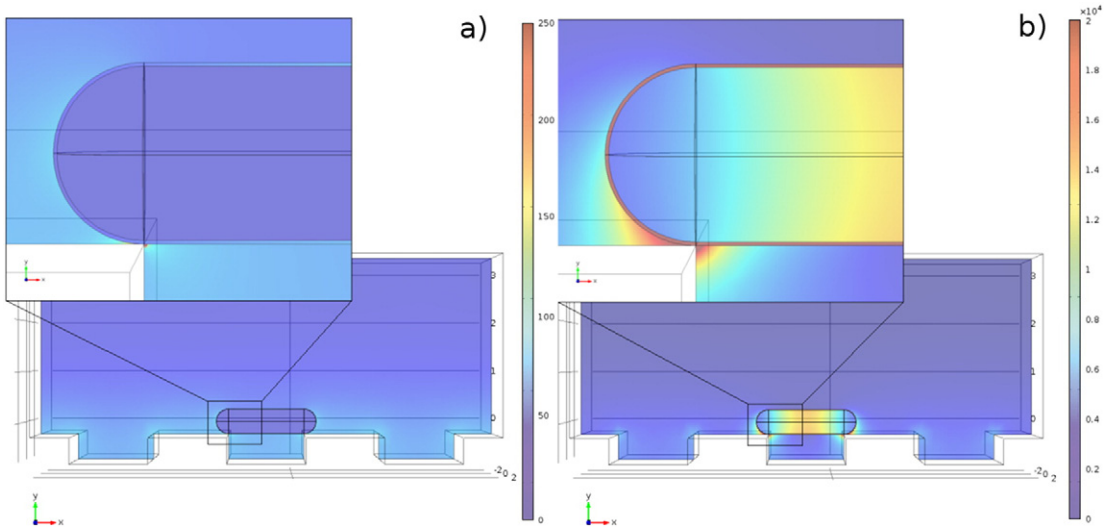

Fig. 2. Current density representation ($A \cdot m^2$) of the simulated model at 1 kHz (a) and 1 MHz (b).

as above. The corresponding spectrum in Fig. 3 b shows an increase of impedance in the low frequency range, as expected. This result is in accordance with those obtained for capacitive biosensors [22], where a decrease in capacitance is monitored due to antibody–antigen interactions taking place at the interface. Silica beads, which are dielectric particles, were deposited at the surface of the electrodes by precipitation from a suspension in deionized water. A bead density of $8.1 \cdot 10^5$ beads/mm^2 on the IDE surface was estimated by bead counting using an optical microscope. The impedance spectrum was measured in the same solution as above before and after silica bead deposition. The presence of the beads on the IDE surface does not significantly alter the impedance at low frequencies. This can be explained by the fact that they only block the electrode-solution interface at a single point of contact. Therefore, if the cells were cylindrical particles like those simulated, they would only contact the IDE surface on a single point or a line, and the effect on the interface impedance would be similar to that of the silica beads. The only feasible explanation for that impedance increase in the low frequency range is that the *E. coli* adhered covering a significant area of the IDE surface, this being likely related to the stress conditions to which they are submitted, as explained above, and thus showing a similar effect on the spectra to that due to the adsorption of proteins.

4. Conclusion

The impedance analysis of the bacteria interaction with Ab-modified IDEs was carried out using the so-called differential impedance spectra approach, instead of the widespread fitting to an EEC, and this permits to detect the bacteria unique electrical fingerprint. This fingerprint is directly related to the cell structure and it is demonstrated to be different to the impedance fingerprints of other events that may take place when an IDE is immersed in a solution whose conductivity changes, an IDE whose surface is blocked by a protein like BSA or interacted with insulating particles such as silica beads.

Overall, we believe that the direct impedimetric detection of bacteria by assessing its unique fingerprint shows the potential to be applied as a simple, specific and rapid detection scheme in the development of novel label-free electrochemical analytical devices for bacteria.

Acknowledgments

One of the authors (M.M.-A) acknowledges the MINECO Spanish Ministry for the fellowship BES-2011-044209.

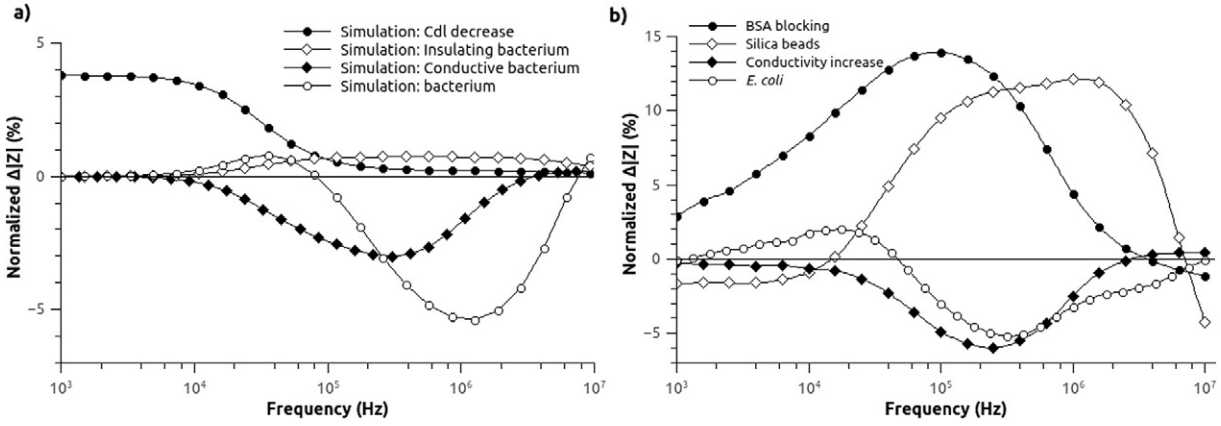

Fig. 3. Comparison between simulations and experimental increment of impedance across all frequency range: (a) Data from COMSOL simulations for an increase of interface conductance and the alteration due to a decrease in the interface capacitance of $5 \cdot 10^{-4}$ F/m^2 and due to the presence of different bacterium-shaped objects: entirely insulating, entirely conductive and with three-shell model parameters. (b) Experimental data for the measurement of different events which affect differently the impedance: the addition of 1 μm-diameter silica beads, the blocking of IDEs surface with BSA protein, an increase of conductivity of 3 μS/cm and bacterial specific attachment (measurement at time = 30 min).

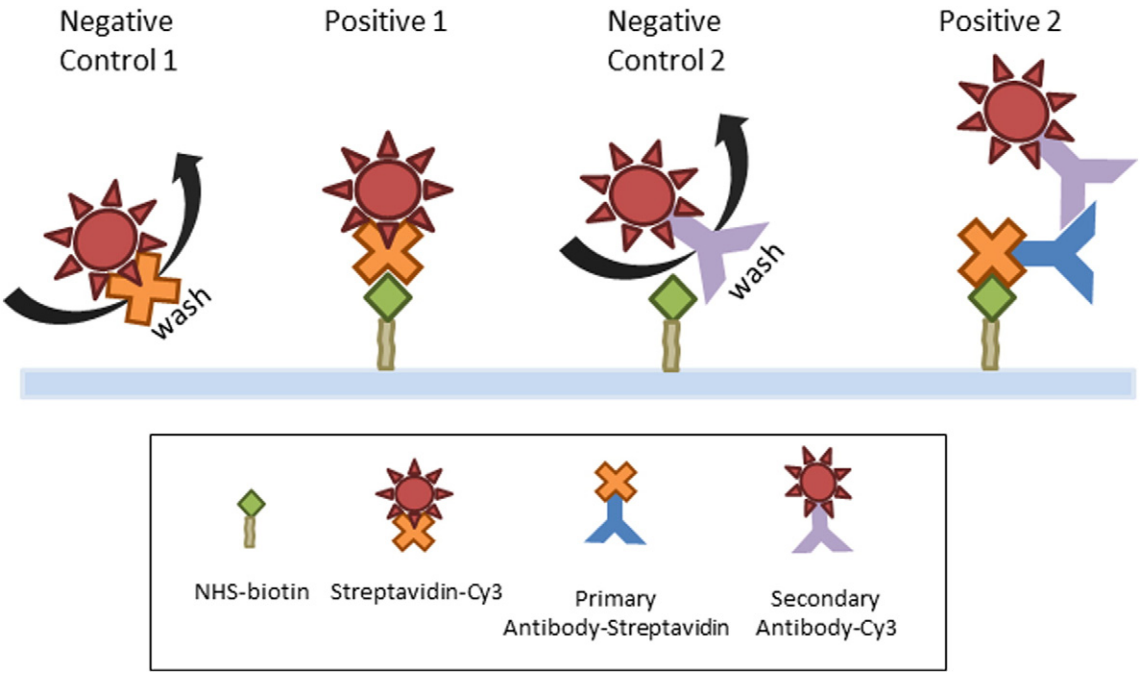

Fig. A.1. Scheme of the four different treated surfaces. Negative controls are expected not to be fluorescent due to the lack of specific union of Cy3-reagents.

Appendix A. IDE surface functionalization

Polysilicon IDEs were coated with an antibody to *E. coli* using the protocol described in the experimental section of the paper. In order to evaluate the successful antibody functionalization, a thorough characterization of every step of the set protocol was carried out by fluorescence imaging.

The functionalization protocol included the following steps:

1. polysilicon activation by oxygen plasma;
2. introduction of amine groups by a silanization process with APTMS;
3. covalent attachment of the Biotin-PEG_{12}-NHS derivative to the amine moieties; and
4. antibody coating using an anti-*E.coli* –streptavidin conjugate.

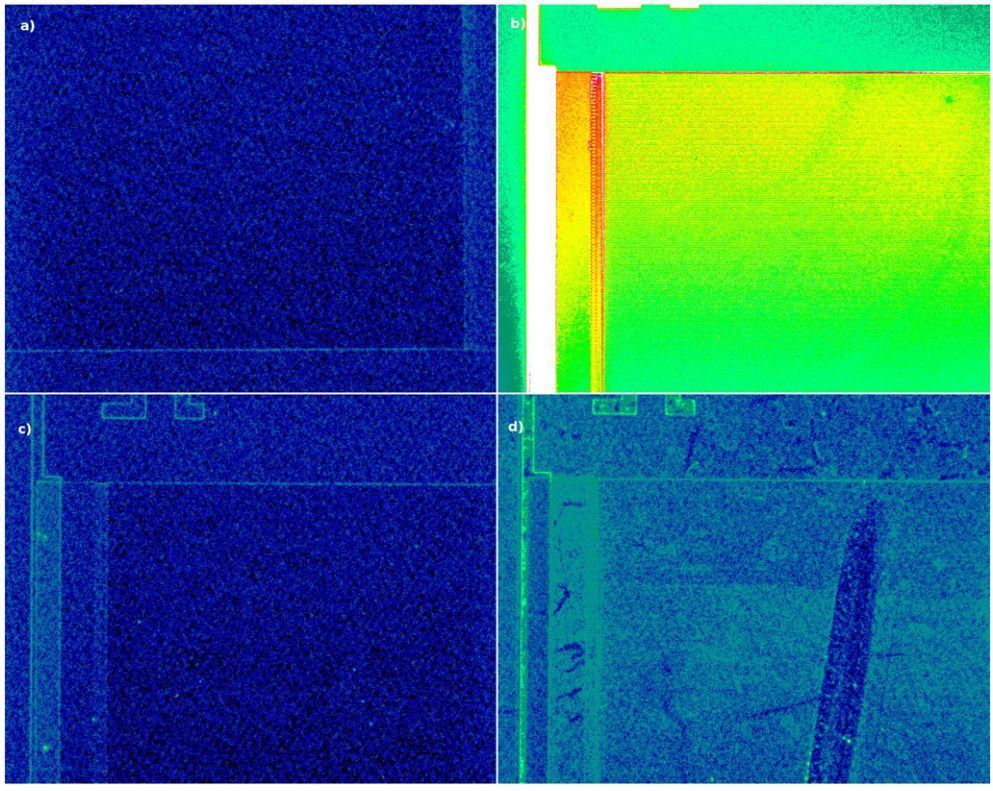

Fig. A.2. Fluorescence of 4 IDE chips modified as described in the text. Negative control 1 without biotin (a); positive control 1 with biotin (b); negative control 2 without anti-*E.coli* antibody (c); and positive control 2 with anti-*E.coli* antibody (d).

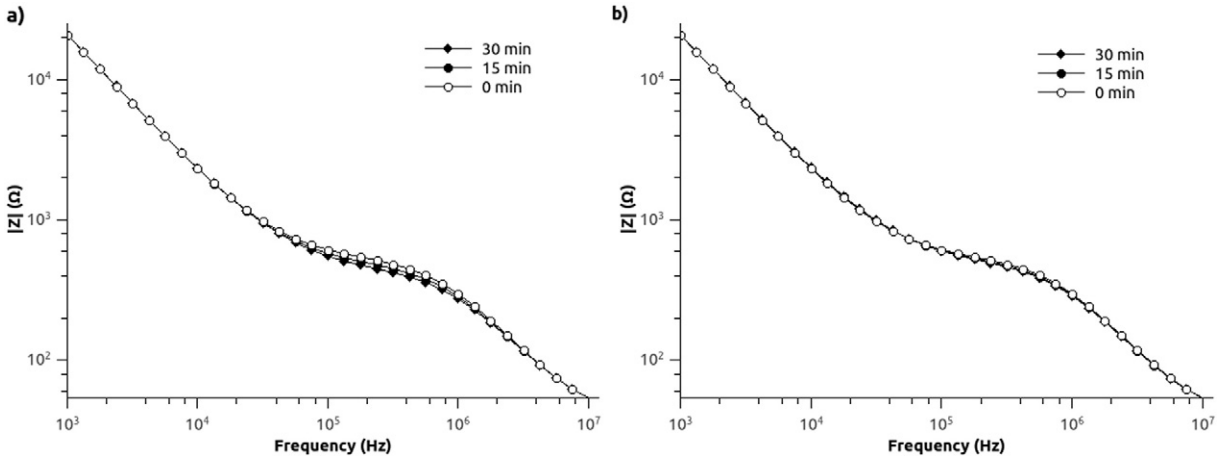

Fig. B.1. Bode plot for experimental data (a), and Bode plot for refined data having compensated conductivity changes.

Biotin covalent attachment was tested using a Cy3–streptavidin conjugate (Sigma-Aldrich). Four silanized polysilicon IDE chips not coated with biotin (negative control 1) and four chips coated with biotin (positive control 1) were incubated for 30 min at room temperature in 20 μg/mL of Cy3-streptavidin. A scheme of these reactions is shown in Fig. A.1.

In parallel, anti-*E.coli* antibody attachment to the biotinylated IDE surface was checked using an anti-IgG anti-*E. coli* secondary antibody labeled with Cy3 (Cy3-Ab to goat IgG from KPL). Four biotinylated IDE chips (negative control 2) and four chips coated with anti-*E. coli* IgG (positive control 2) were incubated for 30 min at room temperature in 10 μg/mL of Cy3-IgG conjugate. A scheme of these reactions is also shown in Fig. A.1.

All the chips were rinsed successively with PB-T (100 mM phosphate buffer containing 0.05% Tween pH 7) and water and finally dried under a nitrogen stream. Fig. A.2 shows fluorescent images of one chip of each group.

Fluorescent results were processed and analyzed using Image J free software (USA) [23] and Deducer data analysis program [24].

Applying a Welch Two Sample T-test considering both negative controls and both positive samples as two groups of population, it is concluded that the difference between groups is statistically significant (p-value = 0).

Therefore, this study clearly shows that both reactions, that are biotin attachment and anti-*E.coli* antibody interaction with the biotinylated surface, did take place, thereby attaining the anti-*E.coli* functionalization of the IDE chips.

Appendix B. Conductivity correction

Conductivity was recorded during bacterial impedimetric measurements. Fig. B.1 a represents Bode plot of one experimental data with a conductivity increment due to bacterial metabolic activity; its conductivities being of 30.7 μS/cm at 0 min, 34.6 μS/cm at 15 min and 37.6 μS/cm at 30 min.

A conductivity calibration was carried out for each electrode and a linear regression at every frequency measured was performed based on this calibration. Impedance variation due to conductivity increment was calculated for each experimental conductivity and subtracted to experimental data. These refined data only considers impedance variation caused by bacterial presence on IDE surface without the noise produced by conductivity increment. Fig. B.1 b shows Bode plot for refined data.

References

[1] M. Kim, T. Jung, Y. Kim, C. Lee, K. Woo, J.H. Seol, et al., A microfluidic device for label-free detection of *Escherichia coli* in drinking water using positive dielectrophoretic focusing, capturing, and impedance measurement, Biosens. Bioelectron. 74 (2015) 1011–1015, http://dx.doi.org/10.1016/j.bios.2015.07.059.
[2] A. Shabani, C.A. Marquette, R. Mandeville, M.F. Lawrence, Modern probe-assisted methods for the specific detection of bacteria, J. Biomed. Sci. Eng. 08 (2015) 104–121, http://dx.doi.org/10.4236/jbise.2015.82011.
[3] A. Ahmed, J.V. Rushworth, N.A. Hirst, P.A. Millner, Biosensors for whole-cell bacterial detection, Clin. Microbiol. Rev. 27 (2014) 631–646, http://dx.doi.org/10.1128/CMR.00120-13.
[4] J.E. Line, N.J. Stern, B.B. Oakley, B.S. Seal, Comparison of an automated most-probable-number technique with traditional plating methods for estimating populations of Total aerobes, coliforms, and *Escherichia coli* associated with freshly processed broiler chickens, J. Food Prot. 74 (2011) 1558–1563, http://dx.doi.org/10.4315/0362-028X.JFP-11-024.
[5] D. Bonilla, M. Mallén, R. de la Rica, C. Fernández-Sánchez, A. Baldi, Electrical readout of protein microarrays on regular glass slides, Anal. Chem. 83 (2011) 1726–1731, http://dx.doi.org/10.1021/ac102938z.
[6] A. Ahmed, J.V. Rushworth, J.D. Wright, P.a. Millner, Novel impedimetric immunosensor for detection of pathogenic bacteria streptococcus pyogenes in human saliva, Anal. Chem. 85 (2013) 12118–12125, http://dx.doi.org/10.1021/ac403253j.
[7] A. Buckland, S. Kessock-Philip, S. Bascomb, Early detection of bacterial growth in blood culture by impedance monitoring with a Bactometer model 32, J. Clin. Pathol. 36 (1983) 823–828, http://dx.doi.org/10.1136/jcp.36.7.823.
[8] H. Etayash, K. Jiang, T. Thundat, K. Kaur, Impedimetric detection of pathogenic gram-positive bacteria using an antimicrobial peptide from class IIa bacteriocins, Anal. Chem. 86 (2014) 1693–1700, http://dx.doi.org/10.1021/ac4034938.
[9] G. Kim, J.-H. Moon, M. Morgan, Multivariate data analysis of impedimetric biosensor responses from *Salmonella typhimurium*, Anal. Methods 5 (2013) 4074, http://dx.doi.org/10.1039/c3ay40256h.
[10] K. Settu, C.-J. Chen, J.-T. Liu, C.-L. Chen, J.-Z. Tsai, Impedimetric method for measuring ultra-low *E. coli* concentrations in human urine, Biosens. Bioelectron. 66 (2015) 244–250, http://dx.doi.org/10.1016/j.bios.2014.11.027.
[11] R. De La Rica, C. Fernández-Sánchez, A. Baldi, Electric preconcentration and detection of latex beads with interdigitated electrodes, Appl. Phys. Lett. 90 (2007)http://dx.doi.org/10.1063/1.2731311.
[12] S.M. Radke, E.C. Alocilja, A high density microelectrode array biosensor for detection of *E. coli* O157:H7, Biosens. Bioelectron. 20 (2005) 1662–1667, http://dx.doi.org/10.1016/j.bios.2004.07.021.
[13] R. de la Rica, A. Baldi, C. Fernández-Sánchez, H. Matsui, Selective detection of live pathogens via surface-confined electric field perturbation on interdigitated silicon transducers, Anal. Chem. 81 (2009) 3830–3835, http://dx.doi.org/10.1021/ac9001854.
[14] X. Dominguez-Benetton, S. Sevda, K. Vanbroekhoven, D. Pant, The accurate use of impedance analysis for the study of microbial electrochemical systems, Chem. Soc. Rev. 41 (2012) 7228–7246, http://dx.doi.org/10.1039/c2cs35026b.
[15] M. Varshney, Y. Li, Interdigitated array microelectrode based impedance biosensor coupled with magnetic nanoparticle-antibody conjugates for detection of *Escherichia coli* O157:H7 in food samples, Biosens. Bioelectron. 22 (2007) 2408–2414, http://dx.doi.org/10.1016/j.bios.2006.08.030.
[16] R. de la Rica, C. Fernández-Sánchez, A. Baldi, Polysilicon interdigitated electrodes as impedimetric sensors, Electrochem. Commun. 8 (2006) 1239–1244, http://dx.doi.org/10.1016/j.elecom.2006.05.028.
[17] H.K. Hunt, C. Soteropulos, A.M. Armani, Bioconjugation strategies for microtoroidal optical resonators, Sensors (Basel). 10 (2010) 9317–9336, http://dx.doi.org/10.3390/s101009317.
[18] K. Cheung, S. Gawad, P. Renaud, Impedance spectroscopy flow cytometry: on-chip label-free cell differentiation, Cytometry. A. 65 (2005) 124–132, http://dx.doi.org/10.1002/cyto.a.20141.
[19] W. Bai, K.S. Zhao, K. Asami, Dielectric properties of *E. coli* cell as simulated by the three-shell spheroidal model, Biophys. Chem. 122 (2006) 136–142, http://dx.doi.org/10.1016/j.bpc.2006.03.004.

[20] S.M. Chekabab, J. Paquin-Veillette, C.M. Dozois, J. Harel, The ecological habitat and transmission of *Escherichia coli* O157:H7, FEMS Microbiol. Lett. 341 (2013) 1–12, http://dx.doi.org/10.1111/1574-6968.12078.
[21] X. Muñoz-Berbel, N. Vigués, a.T. a Jenkins, J. Mas, F.J. Muñoz, Impedimetric approach for quantifying low bacteria concentrations based on the changes produced in the electrode-solution interface during the pre-attachment stage, Biosens. Bioelectron. 23 (2008) 1540–1546, http://dx.doi.org/10.1016/j.bios.2008.01.007.
[22] M. Labib, M. Hedström, M. Amin, B. Mattiasson, A multipurpose capacitive biosensor for assay and quality control of human immunoglobulin G, Biotechnol. Bioeng. 104 (2009) 312–320, http://dx.doi.org/10.1002/bit.22395.
[23] C.A. Schneider, W.S. Rasband, K.W. Eliceiri, NIH image to ImageJ: 25 years of image analysis, Nat. Methods 9 (2012) 671–675, http://dx.doi.org/10.1038/nmeth.2089.
[24] R. R Development Core Team, R: a language and environment for statistical computing, r found, Stat. Comput. 1 (2014) 409, http://dx.doi.org/10.1007/978–3-540-74686-7.